URSI GASS 2020, Rome, Italy, 29 August - 5 September 2020

Updating IRI Model Using Vertical Sounding and GIM TEC Data and Its Application for the Ekaterinburg HF Radar Data Simulation

Alexey V. Oinats * (1), Ilya K. Edemsky(1), Denis D. Rogov(2)
(1) Institute of Solar-Terrestrial Physics, Irkutsk, Russian Federation, oinats@iszf.irk.ru
(2) Arctic and Antarctic research institute, Saint-Petersburg, Russian Federation

Abstract

We test a technique for region-based updating IRI-family ionosphere models using vertical sounding (VS) and global navigation satellite systems (GNSS) data. As input parameters we used critical frequencies (foF2) obtained at VS stations located in the Ekaterinburg HF radar (EKB; 56.4°N, 58.5°E) field-of-view (FOV) and total electron content (TEC) from CODE global ionospheric maps (GIMs). Updated vertical profiles of electron density are used to simulate HF ground backscatter (GB) in the framework of waveguide approach. We compare simulated HF ground backscatter range-time-intensity (RTI) with observed one by the EKB HF radar to test effectiveness of various updating schemes.

1 Introduction

There is a number of empirical ionosphere models which can be used for HF waves propagation simulation. These models predict monthly median ionosphere state and are suitable for long-term HF propagation forecast. HF propagation characteristics calculated under long-term forecast may significantly differ from observed ones. This represents day-to-day (or even hour-to-hour) variability of the ionosphere. On the other hand, knowing how HF waves propagated is often important for improving interpretation of observational data and/or for increasing accuracy of determination of secondary characteristics, such as, parameters of ionospheric disturbances. One way to bring HF simulation closer to observations is updating median ionosphere model using real measurements.

In the report we test a technique for region-based updating IRI-family ionosphere models, such as IRI-2012 [1] and IRI-PLAS [2], using data of vertical sounding (VS) and global navigation satellite systems (GNSS). As input parameters we used critical frequency of F2 layer (foF2) obtained at VS stations (Arti, Amderma, Salekhard, Dikson, and Norilsk) located in the Ekaterinburg HF radar (EKB; 56.4°N, 58.5°E) field-of-view (FOV) and total electron content (TEC) from global ionospheric maps (GIMs). The locations of the radar, its FOV, and VS stations are shown in Figure 1. Updated vertical profiles of electron density are used to simulate HF GB characteristics in the framework of waveguide approach. We compare simulated HF GB range-time-intensity (RTI) with the observed one by the EKB HF radar to test effectiveness of various updating schemes.

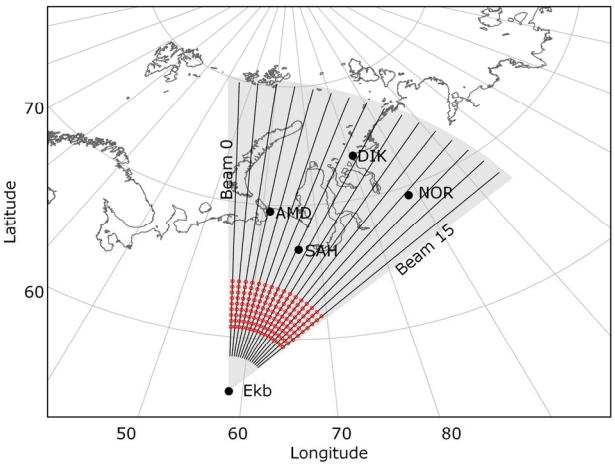

Figure 1. The EKB HF radar location and its FOV. Vertical ionosonde locations are shown by black circles with labels

2 Technique for IRI Model Updating

For purposes of HF propagation simulation we need to know a spatial distribution of the electron density along the propagation path. Critical frequency, foF2, has the greatest impact on the HF propagation, and, therefore, it should be corrected (updated) first. One of the advantages of IRI model is a built-in mode in which electron density height profile can be adjusted by user input foF2 value. If one have a set of foF2 measured in spatially separated points for a given time moment, it becomes possible to make a spatial interpolation of the measured values (or their deviations from the model values). Then foF2 values interpolated along a given propagation path can be used as input to calculate updated IRI electron density profiles.

In this study we check three schemes for IRI model updating. In the first one we used foF2 measured by VS to calculate a correction factor which is equal to the ratio of the observed critical frequency to the model one at the ionosonde location

$$r = \frac{foF2_{obs}}{foF2_{model}}. \quad (1)$$

For a set of VS stations we have a set of correction factors spatially distributed in the region under analysis. The factors are interpolated using inverse weighted distance interpolation methods [3, 4] modified for the spherical

case. At a point of interest the actual critical frequency can be obtained via the correction factor, r_{int}, and the model critical frequency, $foF2'_{model}$, calculated for this point.

$$foF2_{calc} = r_{int} \cdot foF2'_{model}. \quad (2)$$

The second scheme uses GIM TEC maps and IRI-PLAS model [2] for calculation the actual foF2 in a given point. We used GIM maps provided by Center for Orbit Determination in Europe (CODE) [5]. The CODE maps are generated on a daily basis using TEC data from about 200 GPS/GLONASS sites of the International GNSS Service (IGS) and other institutions. The CODE TEC maps have a spatial resolution of 2.5°×5° in the geographic latitude and longitude, and time resolution of 2 hours.

IRI-PLAS electron density profile below F2 layer peak coincides with the IRI profile which is based on well-known global ionospheric maps CCIR and URSI. Above F2 layer peak the profile is calculated using the IZMIRAN plasmasphere model, which was developed based on in-situ electron density measurements provided by Canadian satellites ISIS1 and ISIS2, and Russian Intercosmos-19 [6]. A feature of IRI-PLAS is a built-in mode, in which both foF2 and hmF2 (F2 layer peak height) can be updated according to user input TEC value.

In the second scheme, first of all, we interpolate GIM TEC in temporal (by linear interpolation between two neighboring UTs) and spatial domains (by inverse weighted distance interpolation [4]) to get TEC value which corresponds to a given UT and given coordinates. Then we used IRI-PLAS model [2] to calculate $foF2_{calc}$ corresponding to the TEC value at a point of interest.

The third scheme uses foF2 measured at VS station and GIM TEC together. The combined use of actual foF2 and TEC_{GIM} values allow us to make some calibration of the equivalent ionosphere slab thickness [7] provided by IRI-PLAS. First, we calculate the "observed" slab thickness for each VS station

$$\tau_{obs} = \frac{TEC_{GIM} \cdot 10^3}{1.24 foF2_{obs}^2}. \quad (3)$$

Then the proportionality coefficient is calculated between τ_{obs} and τ_{model} for VS station location

$$r_\tau = \frac{\tau_{obs}}{\tau_{model}}. \quad (4)$$

Spatial interpolation of r_τ is applied then to correct IRI-PLAS slab thickness at a point of interest. The corrected foF2 are calculated at this point in the following way

$$foF2_{calc} = 8.97 \sqrt{\frac{TEC_{GIM}}{r_{obs}\tau_{model}}}. \quad (5)$$

All the schemes described above allow us to reconstruct "actual" foF2 at each point of a given HF propagation path. To calculate electron density profiles which are necessary for subsequent HF propagation simulation we use $foF2_{calc}$ as user input to IRI-2012 model [1].

3 Technique for HF Ground Backscatter Amplitude Simulation

The technique we used for the HF GB simulation [8, 9] is based on adiabatic approach of eigenfunction method [10]. In case of azimuthally symmetric Earth-ionosphere waveguide electromagnetic field induced by arbitrary emitter is expressed by a series of eigenfunctions as

$$E(\vec{r},t) \sim Re\left\{\sum_n I_n(\varphi) A_n(\vec{r}) g_0\big(t - \tau_n(\vec{r})\big) e^{i\Phi_n(\vec{r}) - i\omega_0 t}\right\}. \quad (6)$$

Where $\tau_n(\vec{r})$, $A_n(\vec{r})$ and $\Phi_n(\vec{r})$ are the time lag, amplitude and phase of eigenfunction with number n respectively, $g_0(t)$ is envelope of the transmitted signal, ω_0 is a cycle frequency. Excitation coefficient $I_n(\varphi)$ is related with the characteristics of emitter, or with scattering properties of rough ground surface. In the latter case the relation can be expressed as,

$$I_n(\varphi) \sim A_i(r_s) \sqrt{\frac{\sigma(\alpha_i,\alpha_s) S \cos(\alpha_i)}{4\pi}}. \quad (7)$$

Where $\sigma(\alpha_i, \alpha_s)$ is a scattering coefficient, $A_i(r_s)$ is an incidence HF field amplitude on the surface, α_i and α_s are the incidence and scattering angles accordingly, S is an area of scattering region at certain time moment. We used an analytical expression for scattering coefficient derived by small perturbation method [11]

$$\sigma(\alpha_i,\alpha_s) \sim k^4 \cos^2(\alpha_i)\cos^2(\alpha_i) W(-k(\sin(\alpha_i) + \sin(\alpha_i))). \quad (8)$$

Where k is a wave number and $W(x)$ is one dimensional spectral density of roughness height distribution.

4 EKB HF GB Observation and Simulation

Figure 2a shows RTI plot obtained by the EKB HF radar on beam #1 (azimuth -1.06°) during February 8, 2014. Universal time (UT) is shown on the horizontal axis. The date is characterized by moderate geomagnetic activity during the first half of the day (Ap=23). GB intensity is shown by color according to the right-side color bar. Red crosses show GB echoes with maximum intensity for a given UT. As we can see from Figure 2a there is a distinct track corresponding to the scattering near the HF skip distance. The track is located near ranges of ~1000 km, and it is characterized by a typical diurnal behavior.

Corresponding HF GB intensity simulations are presented in Figures 2b–2e. Calculated intensity is shown by color according to the right-side color bar. Black crosses show minimum slant range for a given UT. As one can see there is a significant difference in the absolute values of the observed and simulated intensity. The observed intensity is calculated with relation to the measured HF noise level (i.e., this is the signal-to-noise ratio), but in the simulation the intensity is reduced to a level of 1 volt. Further we discuss the differences and similarities of the observed and simulated results regardless of the absolute intensity values.

Figure 2b shows GB intensity calculated using the original (basic) IRI-2012 model without updating. In general application of basic IRI-2012 allows to reproduce satisfactorily the diurnal behavior of the HF GB as compared with the observations. However there are at least two significant differences between the observed and simulated results. First, simulation systematically overestimates minimum slant range as compared with the observations. Second, simulation show somewhat different diurnal trend of minimum slant range. In other words overestimation after the noon hours is greater than before these hours.

Figure 2c shows GB intensity calculated using the IRI-2012 model updated by VS data only according to the first scheme described in Section 2. In comparison with Figure 2b the adaptation by VS significantly decreases difference between observed and simulated minimum slant range. The intensity track becomes wider in slant ranges which better corresponds to the observations. In addition there is a sharp vanish of HF GB at about 13:30 UT as it also seen in Figure 2a.

Figure 2d shows the results of calculation using the IRI-2012 model updated by GIM TEC data only according to the second scheme described in Section 2. We can see that adaptation using GIM TEC also significantly overestimates minimum slant range. However there is some correction to its diurnal trend as compared with Figure 2a.

Figure 2e shows the results of calculation using the IRI-2012 model updated by combined VS and GIM TEC data according to the third scheme described in Section 2. Comparing Figures 2b and 2e, one can see close similarity between them. The difference is seen mainly for the time interval from 15 till 17 UT. Figure 2e does not show any intensity during this interval unlike Figure 2b.

Figure 3 shows relative average diurnal deviation between observed and calculated minimum slant ranges for different radar beams. The beams are characterized by different azimuths. Beam #0 has azimuth of -4.3°, whereas beam #15 directed to the azimuth of 44.3°. Deviations for different updating schemes are shown by different colors. Black, red, blue, and green colors

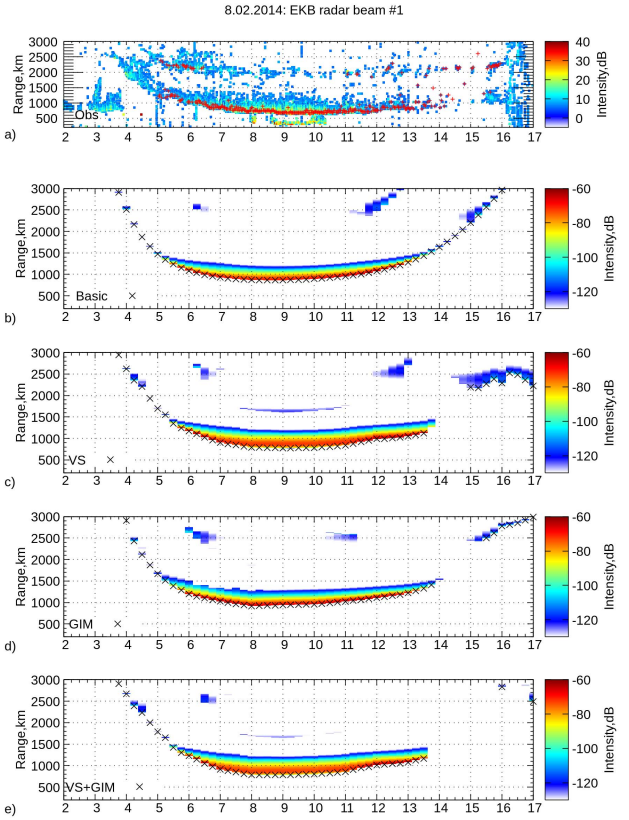

Figure 2. Pannel (a) - the EKB HF radar range-time-intensity plot (RTI) observed on Febraury 8, 2014 on beam #1. Pannels (b), (c), (d), and (e) ground backscatter intensity simulated without updating (basic), VS only, GIM only, and VS + GIM updating schemes

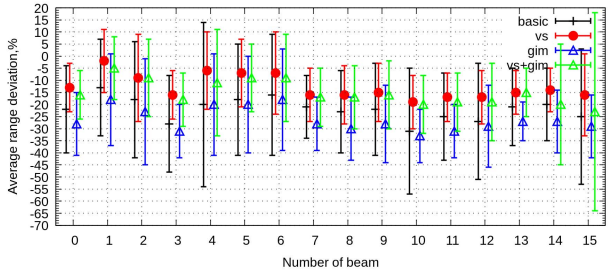

Figure 3. Relative average deviation and standard deviation of simulated minimum HF ground backscatter range without updating (black), VS only (red), GIM only (blue), and VS + GIM (green)

correspond to original (basic) IRI-2012, updated by VS only, GIM only, and combined VS + GIM accordingly. Relative standard deviation is also shown in Figure 3 by vertical bars.

As one can see relative deviation (and standard deviation) is different for different beams. In case of original IRI-2012 (without updating) the greatest deviation of -31% (with standard deviation of ±26%) is seen for beam #10. The lowest deviation of -13% (with standard deviation of ±20%) is seen for beam #1. It is well known that IRI

accuracy becomes worse with latitude increase starting from subpolar regions. However the behavior of deviation described above represents some kind of IRI-2012 accuracy anisotropy in the geographical region under analysis.

In comparison with basic IRI-2012 adaptation by VS foF2 significantly decreases the deviation: to -19% (with standard deviation of ±11%) and to -2% (with standard deviation of ±13%) for beams #10 and #2 accordingly. In addition the deviation distribution over azimuths becomes more uniform, reflecting spatial distribution of VS stations used for updating. Updating by GIM TEC data does not decrease the average deviation, but decreases the standard deviation almost twice in comparison with basic IRI-2012.

In comparison with the updating by VS foF2, the third scheme, using combined VS and GIM data, leads to somewhat greater deviations (and standard deviations). However for beams #14 and #15 the standard deviation increased dramatically, and it becomes greater even than basic IRI-2012 deviation. Thus application of the combined scheme (VS+GIM) is reasonable only in case of VS data lack.

5 Conclusion

We test IRI model updating technique using VS and GIM TEC data in application to HF ground backscatter simulation. Comparison of three updating schemes shows the better effectiveness of VS updating scheme in comparison with updating by GIM TEC. Combined VS and GIM data does not improve correspondence between observations and simulation. However the combined scheme can be useful in the regions where there is a lack of VS stations.

Application of the presented updating technique is perspective for improving interpretation of HF radar data.

6 Acknowledgements

The reported study was funded by RFBR, project number 19-05-00889 and project number 19-02-00513. The results were obtained using the equipment of Center for Common Use «Angara» http://ckp-rf.ru/ckp/3056/. We are grateful to the CODE team for the access to GIM TEC data provided from the CODE FTP directory: ftp://ftp.aiub.unibe.ch/CODE/.

7 References

1. D. Bilitza, D. Altadill, V. Truhlik, V. Shubin, I. Galkin, B. Reinisch, and X. Huang, "International Reference Ionosphere 2016: From ionospheric climate to real-time weather predictions," *Space Weather*, **15**, 2017, pp. 418–429, doi:10.1002/2016SW001593.

2. T.L. Gulyaeva, D. Bilitza, "Towards ISO Standard Earth Ionosphere and Plasmasphere Model," *In: New Developments in the Standard Model*, NOVA Publishers, 2012.

3. D. Shepard, "A two dimensional interpolation function for irregularly spaced data," *Proc. 23rd Nat. Conf.*, 1968, pp. 517-524.

4. R. Franke, G. Neilson, "Smooth interpolation of large sets of scattered data," *International Journal of Numerical Methods in Engineering*, **15**, 1980, pp. 1691–1704.

5. S. Schaer, "Mapping and predicting the Earth's ionosphere using the global positioning system," Ph.D. dissertation, Astron. Inst. Univ. of Bern, Switzerland, 1999.

6. Yu.K. Chasovitin, T.L. Gulyaeva, M.G. Deminov, S.E. Ivanova, "Russian standard model of ionosphere (SMI)," *COST251TD(98)005*, RAL, UK, 1998, pp. 161–172.

7. R.S. Roger, "Measurements of the equivalent slab thickness of the daytime ionosphere," *Journal of Atmospheric and Terrestrial Physics*, **26**, 4, 1964, pp. 475–497.

8. A.V. Oinats, V.I. Kurkin, K.A. Kutelev, N. Nishitani, "The outlook of SuperDARN radars application for monitoring of the ionospheric dynamics in Russia," *Physical Bases of Instrumentation*, **1**, 3, 2012, pp. 3-18 (in Russian).

9. S. N. Ponomarchuk, N. V. Ilyin, V. V. Khakhinov, V. I. Kurkin, A. V. Oinats, and M. S. Penzin "Comprehensive algorithm for calculation of backscatter signals characteristics within the waveguide approach," *Proc. SPIE 11208, 25th International Symposium on Atmospheric and Ocean Optics: Atmospheric Physics*, 112088R, 18 December 2019, https://doi.org/10.1117/12.2539946.

10. V.I. Kurkin, I.I. Orlov, V.N. Popov, "Normal Wave Technique in HF Radio Communication Problem," Nauka, Moscow, 1981.

11. A. Isimaru, "Wave Propagation and Scattering in Random Media," Mir, Moscow, 1981.